Controlled Mobile Radiation Detection Under Stochastic Uncertainty

Indrajeet Yadav and Herbert G. Tanner

***Abstract*—Building upon recent insights on the effect of sensor mobility on the detection performance of mobile radiation sensors, this paper analyzes the impact of stochastic noise in the motion of the sensors on their decision-making accuracy. A stochastic optimal control law for the sensors is designed to maximize decision-making performance. Numerical simulations indicate that noisy sensor motion significantly reduces decision-making accuracy, and is especially detrimental to the detection of weak radioactive sources.**

***Index Terms*—Radiation Detection using Mobile Sensors, Stochastic Optimal Control, Pontryagin's Maximum Principle.**

I. INTRODUCTION

MOST advanced radiation detection algorithms proposed for detecting nuclear material in motion are based on deploying a distributed network of *static* sensors, and fusing of their data to estimate aspects of the target in question [9], [10]. The principle behind all these algorithms is to distinguish the signal (in terms of counts of source gamma-rays hitting the detector) from the noise (counts due to background radiation). Fusing data from a *collection of sensors* aims at increasing the overall Signal-to-Noise-Ratio (SNR) [7], and eventually improve detection performance.

Radiation detection algorithms rest on the hypothesis that the statistics of radioactive source gamma-rays incident on a detector is that of an inhomogenous Poisson process [12]. Due to the strong dependence of the process intensity on the distance between sensor and source (inverse square law [7]), one way to further increase SNR is to exploit sensor mobility: move the sensors as close to the source as possible. In that vein, Ma et al. optimize threat-based coverage to a given search area by allowing limited mobility to the sensors [5]. Ristic et al., on the other hand, utilize a mobile sensor in an information gain-driven search for high intensity radioactive sources [11]. Neither case, however, focuses on the effect of sensor mobility—and position uncertainty, in particular—on detection performance.

Pahlajani et al. formulate the mobile detection problem as a Likelihood Ratio Test (LRT) within the Neyman-Pearson framework. They *analytically* obtain (Chernoff) bounds on error probabilities in terms of sensor mobility (specifically, the relative distance between the source and the sensor) [8]. Using these analytical bounds as proxies for the otherwise intractable true error probabilities, Sun et al. [13] derive an optimal steering law for the sensors that maximizes the decision-making accuracy of the network. This is a formal proof that driving the sensor close to the source as quickly as possible is indeed the optimal sensor motion strategy in terms of improving decision-making accuracy.

All aforementioned work deals with the case where both sensor and source motion is *deterministic*. In applications, however, there is inherent variability in motion—one reason could be environmental disturbances. A question of practical relevance, therefore, is to what extent the decision-making accuracy is affected by stochastic noise in sensor motion, and whether the optimal steering strategy for the sensors changes due to noise. The contributions of this paper are in providing answers to these two questions.

The paper approaches the problem of modeling uncertainty in the time-varying distance between sensor and source in the form of a Stochastic Differential Equation (SDE). Building on related earlier work in the deterministic setting, it formulates a *stochastic* optimal control problem using the *Stochastic Maximum Principle* [1], and solves it *analytically* in a single dimension to show that the deterministic optimal sensor motion strategy is also optimal in the stochastic case. A discussion on why the deterministic bounds could be used in a stochastic case without avoiding complicated filtering analysis is presented in Section II. Finally, the paper exposes the effect of the intensity of noise in the measurement of distance between sensor and source, on the effectiveness of the optimal control strategy and the resulting decision-making accuracy regarding the presence of the source.

II. BACKGROUND

This section reviews previous results for deterministic radiation detector (referred to simply as *sensor*) motion [8], [13] and introduces necessary notation for stating an optimal control and decision-making problem in the case when the motion of this sensor is stochastic. The probabilistic setup is as follows. On the measurable space $(\Omega, \mathscr{F})$, there is a counting process N_t, for $t \in [0, T]$. Practically, N_t represents the number of counts recorded at the radiation detector located at position $x \in \mathbb{R}^3$, up to (and including) time $t \in [0, T]$. The sensor position x is observed during the whole interval $[0, T]$.

There are two hypotheses, H_0 and H_1, each expressing a competing opinion as to whether a radiation source is actually present on a platform, referred to as the *target*, which is located at position $y \in \mathbb{R}^3$. The position of the target is assumed to be time-varying in general. Hypothesis H_0 asserts that the target at position y is benign, while hypothesis H_1 states that the

Yadav and Tanner are with the Department of Mechanical Engineering at the University of Delaware {indragt,btanner}@udel.edu

This work has been supported in part by NSF under award # 1548149, and in part by DTRA under grant #HDTRA1-16-1-0039.

target carries a source of radioactivity a (in counts per unit of time).

The two hypotheses H_0 and H_1 correspond, respectively, to two distinct probability measures $\mathbb{P}_0$ and $\mathbb{P}_1$ on $(\Omega, \mathscr{F})$. With respect to measure $\mathbb{P}_0$, the process N_t is a Poisson process with intensity $\beta(t)$; with respect to $\mathbb{P}_1$, however, the same process is assumed to be Poisson with intensity $\beta(t) + \nu(t)$. In the context of the application at hand, $\beta(t)$ is the (possibly time-varying) intensity at time t due to background radiation at x, while $\nu(t)$ represents the intensity of the source (whenever present) as perceived by the sensor at time t. The functions $\beta(t)$ and $\nu(t)$ defined on $[0, T]$ are assumed to be bounded, continuous and strictly positive [8].

Function $\nu(t)$ reflects implicitly the dependence of the source intensity perceived by the sensor on the distance between the sensor and the source. The functional representation used here encodes the inverse square law [7] relationship between range and perceived intensity, and the latter can be time varying because the distance between the two points can change over time. Letting χ denote a cross-section coefficient of the sensor, the perceived intensity is assumed here to be expressed as

$$\nu(t) = \frac{\chi a}{2\chi + \|y - x\|^2} \ . \tag{1}$$

A test for deciding between H_0 and H_1 can be thought of as an event B_1, whose occurrence or non-occurrence can be ascertained on the basis of sensor observations over $[0, T]$, and has the following significance: if outcome $\omega \in B_1$, decide H_1; otherwise, that is if $\omega \in B_0 \triangleq \Omega \setminus B_1$, decide H_0. For such a test, two types of errors can occur. A false alarm occurs if $\omega \in B_1$ with H_0 being the correct hypothesis; this occurs with probability $\mathbb{P}_0(B_1)$. A missed detection (miss) occurs if the outcome $\omega \in B_0$ while H_1 is the true hypothesis; this occurs with probability $\mathbb{P}_1(\Omega \setminus B_1)$.

In this setting, the optimal test for deciding between H_0 and H_1 is an LRT obtained as follows [8]. Let τ_n for $n \geq 1$ denote the n-th jump time (when the sensor generates a count) of N_t, and with the convention that $\prod_{n=1}^{0}(\dots) = 1$, let[1]

$$L_T = \exp\left(-\int_0^T \nu(s)\,\mathrm{d}s\right) \prod_{n=1}^{N_t} 1 + \frac{\nu(\tau_n)}{\beta(\tau_n)} \ . \tag{2}$$

Assume that P_1 is absolutely continuous with P_0, and that H_0 and H_1 are equiprobable [12]. Then for a specific fixed threshold $\gamma > 0$, the test

$$\left\{ L_T \underset{H_0}{\overset{H_1}{\gtrless}} \gamma \right\} \quad \text{where} \quad \gamma \in \mathbb{R} \tag{3}$$

is optimal in the (Neyman-Pearson) sense that if A_2 is any other test whose probability of false alarm $P_0(A_2) \leq P_0(L_T \geq \gamma)$, then the probability of miss for test (3) is at least as low as that for A_2, i.e. $P_1(L_T < \gamma) \leq P_1(\Omega \setminus A_2)$.

For $\mu(t) \triangleq 1 + \frac{\nu(t)}{\beta(t)}$, constant $p \in (0, 1)$, $\eta \triangleq \log\gamma$, and

$$\Lambda(p) \triangleq \int_0^T \left[\, \mu(s)^p - p\,\mu(s) + p - 1 \right] \beta(s)\,\mathrm{d}s \ , \tag{4}$$

[1] L_T is the likelihood ratio [14].

one can express analytically Chernoff bounds on the probability of false alarm P_F and missed detection P_M [8]

$$P_F \leq \exp\left(\, \inf_{p>0}[\Lambda(p) - p\,\eta]\,\right)$$
$$P_M \leq \exp\left(\inf_{p<1}[\Lambda(p) + (1-p)\eta]\right) \ .$$

Let the derivative of (4) (cf. [14, §2.4]) with respect to p be denoted (dependency of μ and β on time is suppressed for clarity)

$$\Lambda'(p) = \int_0^T [\mu^p \log\mu - \mu + 1]\beta\,\mathrm{d}s \ . \tag{5}$$

Now if an upper limit $\alpha > 0$ is set on the bound on probability of false alarm, then there exists a unique solution $p^* \in [0, 1]$ to $\exp\left\{\inf_{p<1}[\Lambda(p) + (1-p)\eta]\right\} = \alpha$ for which the tightest bound on the probability of missed detection is obtained, and the exponent in the bound on the probability of false alarm and missed detection, respectively, is [8]

$$\mathcal{E}_{\mathcal{F}} = \int_0^T [p^*\mu^{p^*}\log\mu - \mu^{p^*} + 1]\beta\,\mathrm{d}s = -\log\alpha \tag{6}$$

$$\mathcal{E}_{\mathcal{M}} = \log\alpha + \Lambda'(p^*) \ . \tag{7}$$

Under noisy sensor motion, the intensity (1) of the source as perceived by the sensor depends on the stochastic process given by $x(t)$; it is therefore a Doubly Stochastic Poisson Process (DSPP) with $x(t)$ in the role of the information process. Typically in DSPP problems, the objective is to estimate the intensity, or infer the parameters of the information process. Treatment of such cases usually necessitates a filtering analysis [12] to yield an estimate of the elusive process intensity. This estimate is then used in lieu of the true intensity which is then to be used in (2)–(3). Stochastic equivalents of (6) and (7) may be calculated via such intricate filtering process [3]. In the case considered here, it is not even clear if very low count rates may even afford such filtering analysis. Here, however, the case is different: the *information process is known*. What is more, by the time T that the decision is to be made, the sample path $x(t)$ is fully observed and known, and consequently so is the intensity ν. There is no need for filtering. For the same reason, the expressions (6) and (7) at time T become true bounds on the probability of false alarm and probability of missed detection, because μ has been observed and is known over the time interval $[0, T]$. Until time T, however, (5) is a random variable. For this reason, and for $t \in [0, T)$, the expressions on the right hands of (6) and (7) are referred to as *prospective bounds*.

Now suppose that the distance between target and sensor, $\|y - x\|$, is regulated by a control input u; thus ν and consequently μ depend implicitly on u. Based on this observation, an optimal control problem can be formulated as follows: *find u that optimizes $\Lambda'(p^*)$ for a given upper limit α on the bound on probability of false alarm.* For the case where $\|y - x\|$ is deterministic, it is known [13] that the optimal sensor management strategy u for sensors is to close the gap between the source and the sensor as quickly as possible. The case where $\|y - x\|$ is random has been an open problem.

III. Stochastic Optimal Sensor Control

Consider a three-dimensional Wiener process W, let $u(t)$ be an $\mathcal{F}_t$-adapted process satisfying $\|u(t)\| \leq u_{\max}$ for all $t \in [0,T]$, denote $\sigma > 0$ the (constant) intensity of stochastic motion disturbances for the sensor, let k be a positive gain, and set δ in the interval $(0, u_{\max}/k)$. Assume that the sensor position, starting at $x(0) = x_0 \in \mathbb{R}^3$, evolves according to

$$\mathrm{d}x = u(t)\,\mathrm{d}t + \sigma\,\mathrm{d}W \qquad \text{if } \|y-x\| > \delta \qquad (8a)$$

$$\mathrm{d}x = -k(y-x)\,\mathrm{d}t + \sigma\,\mathrm{d}W \qquad \text{if } \|y-x\| \leq \delta \qquad (8b)$$

Intuitively, (8) describes the motion of a sensor as a sample path of a switched SDE that has a constant diffusion coefficient and its controllable drift coefficient switches to a proportional control law in the vicinity of the desired operating point, y, which is moving with a speed constrained to $\|\dot{y}\| < u_{\max}$. The latter is intended to keep the sensor close to the target once it has intercepted it, and the particular expression in (8b) is known as the Ornstein-Uhlenbeck (OU) process [2]. In the present setup the sensor motion is modeled as stochastic and the target motion is taken as deterministic, but (8) can be easily reformulated to capture the situation of a stochastic target and a deterministic sensor.

Assuming for simplicity that background radiation is uniform over time, i.e., that β is independent of t, the goal here is to design u in order to improve the accuracy of the binary hypothesis test (3) that is to take place at time T. For that reason a stochastic optimal control problem is formalized. The objective is to minimize with respect to u, subject to (8a) and $u \in \mathcal{U}$, the functional

$$J(u) = \mathbb{E}_{x_0}\left\{ \int_0^T [\mu^p \log \mu - \mu + 1]\beta\,\mathrm{d}s \right\} . \qquad (9)$$

Then, the solution u^* will be applied on (8a) for time $t \in [0, T \wedge T']$, with T' denoting the first exit time from $\|y-x\| > \delta$.

What follows in this section are stochastic extensions of results supporting the deterministic version of the optimal control problem [13], with appropriate modifications.

Corollary 1. *Given u, $\mathbb{E}_{x_0}\{\mathcal{E}_\mathcal{F}\}$ increases strictly with p.*

Proof. Mirrors the deterministic case [13]. □

Corollary 2. *Functional $\mu \mapsto p$, defined implicitly through* (6) *and denoted ϕ, associates to each function $\mu(t)$ a unique p.*

Proof. Mirrors the deterministic case [13]. □

Let $\tilde{\mu}$ be the function obtained due to the perturbation in μ at time instant t. Expressing the perturbation on p due to a perturbation $\tilde{\mu}$ at time t as

$$p(t,\tilde{\mu}) = \phi(\tilde{\mu}) = \phi(\mu) + (\tilde{\mu}-\mu)\left.\frac{\partial p}{\partial \mu}\right|_t$$

and setting $\mathcal{I}_{\mathcal{F}\,\mu\mu} \triangleq \dfrac{\partial^2 (p\,\mu^p \log\mu - \mu^p + 1)\beta}{\partial \mu^2}$, the following lemma can be stated.

Lemma 1.

$$(6) \implies \frac{\partial p}{\partial \mu} = -\frac{p}{\mu \log \mu} .$$

Proof. Pick an arbitrary $t_1 \in [0,T]$. Let $\Delta\mu$ be a (deterministic) needle perturbation on μ at t_1, with duration ϵ, such that $\tilde{\mu}(t) \equiv w \in (1, 1+\frac{a}{2\beta})$ for all $t \in [t_1-\epsilon, t_1]$. Specifically, $\Delta\mu = (w-\mu)\,\Pi_{t_1-\epsilon,t_1}(t)$, where Π denotes the boxcar function.

The Taylor expansion of integrand of $\mathcal{E}_\mathcal{F}$, denoted $\mathcal{I}_\mathcal{F}$, with respect to μ is approximated as

$$\mathcal{I}_\mathcal{F}(\tilde{\mu},\tilde{p}) \approx \mathcal{I}_\mathcal{F}(\mu,p) + \left.\frac{\partial \mathcal{I}_\mathcal{F}}{\partial p}\right|_{t=t_1}\Delta p + \left.\frac{\partial \mathcal{I}_\mathcal{F}}{\partial \mu}\right|_{t=t_1}\Delta\mu + \frac{1}{2}\left.\frac{\partial^2 \mathcal{I}_\mathcal{F}}{\partial \mu^2}\right|_{t=t_1}(\Delta\mu)^2 .$$

Substituting based on $\frac{\partial \mathcal{I}_\mathcal{F}}{\partial \mu} = \beta p^2 \mu^{p-1}\log\mu$, $\Delta p = \frac{\partial p}{\partial \mu}\Delta\mu$, and $\frac{\partial \mathcal{I}_\mathcal{F}}{\partial p} = \beta\,p\,\mu^p\,\log^2\mu$, it follows that

$$\begin{aligned}\mathcal{I}_\mathcal{F}(\tilde{\mu},\tilde{p}) - \mathcal{I}_\mathcal{F}(\mu,p) &= \Delta\mu\left[\beta p^2\mu^{p-1}\log\mu\right]_{t=t_1} + \frac{(\Delta\mu)^2}{2}\left.\frac{\partial^2\mathcal{I}_\mathcal{F}}{\partial\mu^2}\right|_{t=t_1} \\ &\quad + \Delta\mu\left[\beta\,p\,\mu^p\,\log^2\mu\right]_{t=t_1}\left.\frac{\partial p}{\partial\mu}\right|_{t=t_1} .\end{aligned}$$

Integrating the left-hand side over $[0,T]$ will yield the total variation on the bound on the probability of false alarm. Since the latter is constrained by (6) to be $-\log\alpha$, that should be identically zero. The integral of the right-hand side over $[0,T]$ is therefore zero. Solving for $\frac{\partial p}{\partial \mu}|_{t=t_1}$ gives the following expression for this partial derivative:

$$\frac{-\int_0^T \Delta\mu\,\mathrm{d}s\left[\beta p^2\mu^{p-1}\log\mu\right]_{t=t_1} \int_0^T \frac{(\Delta\mu)^2}{2}\,\mathrm{d}s\,\frac{\partial^2\mathcal{I}_\mathcal{F}}{\partial\mu^2}|_{t=t_1}}{\int_0^T \Delta\mu\,\mathrm{d}s\,\left[\beta\,p\,\mu^p\,\log^2\mu\right]_{t=t_1}} .$$

This simplifies slightly to

$$\begin{aligned}\left.\frac{\partial p}{\partial\mu}\right|_{t=t_1} &= -\left[\frac{p}{\mu\log\mu}\right]_{t=t_1} - \frac{\int_0^T \frac{(\Delta\mu)^2}{2}\,\mathrm{d}s\,\frac{\partial^2\mathcal{I}_\mathcal{F}}{\partial\mu^2}|_{t=t_1}}{\int_0^T \Delta\mu\,\mathrm{d}s\,\left[\beta\,p\,\mu^p\,\log^2\mu\right]_{t=t_1}} \\ &= -\left[\frac{p}{\mu\log\mu}\right]_{t=t_1} - \frac{\int_{t_1-\epsilon}^{t_1} \frac{(\Delta\mu)^2}{2}\,\mathrm{d}s\,\frac{\partial^2\mathcal{I}_\mathcal{F}}{\partial\mu^2}|_{t=t_1}}{\int_{t_1-\epsilon}^{t_1} \Delta\mu\,\mathrm{d}s\,\left[\beta\,p\,\mu^p\,\log^2\mu\right]_{t=t_1}} .\end{aligned}$$

As $\epsilon \to 0$, note that $\int_{t_1-\epsilon}^{t_1}\Delta\mu\,\mathrm{d}s \to \epsilon[w-\mu(t_1)]$ and $\int_{t_1-\epsilon}^{t_1}(\Delta\mu)^2\,\mathrm{d}s \to \epsilon[w-\mu(t_1)]^2$. Substituting yields

$$\begin{aligned}\left.\frac{\partial p}{\partial\mu}\right|_{t=t_1} &= -\left[\frac{p}{\mu\log\mu}\right]_{t=t_1} - \left[\frac{\epsilon(w-\mu)^2\,\frac{\partial^2\mathcal{I}_\mathcal{F}}{\partial\mu^2}}{\epsilon(w-\mu)\,\beta\,p\,\mu^p\,\log^2\mu}\right]_{t=t_1} \\ &= -\left[\frac{p}{\mu\log\mu}\right]_{t=t_1} - \left[\frac{(w-\mu)\,\frac{\partial^2\mathcal{I}_\mathcal{F}}{\partial\mu^2}}{\beta\,p\,\mu^p\,\log^2\mu}\right]_{t=t_1} .\end{aligned}$$

Recall that $p = \phi(\mu)$. As the perturbation diminishes, i.e., $w \to \mu$, the second term vanishes and the above reduces to

$$\left.\frac{\partial p}{\partial \mu}\right|_{t=t_1} = -\left[\frac{p}{\mu \log \mu}\right]_{t=t_1} \ .$$

Since $t_1 \in [0, T]$ is arbitrary, the claim is established. □

With that result at hand, the stochastic maximum principle (SMP) [1] can be applied to (9).

A. Stochastic Maximum Principle

Proposition 1. *Whenever it exists, the solution $u^* \in \mathcal{U}$ of* (9) *is*

$$u^*(t) = \frac{y - x}{\|y - x\|} u_{\mathsf{max}} \ . \tag{10}$$

Proof. Under (8a), and noting from Corollary 2 that $p = \phi(\mu) \in (0, 1)$, (9) is expressed as

$$J(u) = \mathbb{E}_{x_0}\left\{\int_0^T \left(\, \mu^{\phi(\mu)} \log \mu - \mu + 1 \,\right) \beta \, \mathrm{d}s\right\} \ .$$

Let $x^*(t)$ denote the optimal state trajectory, $\lambda^*(t)$ be the optimal costate trajectory in the optimal control problem, and $\mu^* \triangleq \mu(x^*)$ for brevity. Then the Hamiltonian is written as

$$H\big(x^*, u^*, \lambda^*\big) = \big[(\mu^*)^{\phi(\mu^*)} \log \mu^* - \mu^* + 1\big]\beta + \lambda^* \, u^* \ . \tag{11}$$

The control $u^*(t)$ is optimal when it minimizes the Hamiltonian (11) for all admissible controls $u \in \mathcal{U}$ [1]. Specifically,

$$H\big(x^*, u^*, \lambda^*\big) \leq H\big(x^*, u, \lambda^*\big) \ .$$

To minimize H, however, the sign of the costate $\lambda^*(t)$ must be known. Given that the control input $u(t)$ *is not a function of* x, the backward stochastic differential equation for the costate for an adapted square integrable process $K(t)$ takes the form [1] (setting $K(t) \equiv K$, $\phi(\mu^*) \equiv \phi^*$ for brevity)

$$\begin{aligned} -\,\mathrm{d}\lambda^*(t) &= \frac{\partial\, \beta[(\mu^*)^{\phi^*} \log \mu^* - \mu^* + 1]}{\partial x^*}\,\mathrm{d}t + K\,\mathrm{d}W \\ &= \frac{\partial\, \beta[(\mu^*)^{\phi^*} \log \mu^* - \mu^* + 1]}{\partial \mu^*}\,\frac{\partial \mu^*}{\partial x^*}\,\mathrm{d}t + K\,\mathrm{d}W \\ &= \beta\left[(\mu^*)^{\phi^*-1}\Big(\mu^* \tfrac{\partial \phi^*}{\partial \mu^*} \log^2 \mu^* + \phi^* \log \mu^* + 1\Big) - 1\right]\tfrac{\partial \mu^*}{\partial x^*}\,\mathrm{d}t \\ &\qquad + K\,\mathrm{d}W \ , \end{aligned}$$

which, by applying Lemma 1 along the optimal trajectory after recalling that $p^* \equiv \phi^*$, the right hand side of the above expression becomes

$$\begin{aligned} &\beta\left[(\mu^*)^{\phi^*-1}\Big(-\frac{\mu^* \log^2 \mu^*\, \phi^*}{\mu^* \log \mu^*} + \phi^* \log \mu^* + 1\Big) - 1\right]\tfrac{\partial \mu^*}{\partial x^*}\,\mathrm{d}t \\ &\qquad + K\,\mathrm{d}W \ = \beta\Big[(\mu^*)^{\phi^*-1} - 1\Big]\tfrac{\partial \mu^*}{\partial x^*}\,\mathrm{d}t + K\,\mathrm{d}W \ . \end{aligned}$$

The costate equation therefore reads

$$\mathrm{d}\lambda^*(t) = -\beta\left[(\mu^*)^{\phi^*-1} - 1\right]\frac{\partial \mu^*}{\partial x^*}\,\mathrm{d}t - K\,\mathrm{d}W$$

with terminal boundary condition on $\lambda^*(T) = 0$ given that there is no terminal cost. A system of forward-backward stochastic differential equations (FBSDEs) can now be written in the optimal state trajectory and costate:

$$\mathrm{d}x^*(t) = u(t)\,\mathrm{d}t + \sigma\,\mathrm{d}W \tag{12a}$$

$$\mathrm{d}\lambda^*(t) = -\beta\left[(\mu^*)^{\phi^*-1} - 1\right]\frac{\partial \mu^*}{\partial x^*}\,\mathrm{d}t - K\,\mathrm{d}W \tag{12b}$$

$$x^*(0) = x_0^* \ , \qquad \lambda^*(T) = 0 \tag{12c}$$

where

$$\frac{\partial \mu^*}{\partial x^*} \overset{(1)}{=} \frac{2\chi a \|y - x^*\|}{\beta\big(2\chi + \|y - x^*\|^2\big)^2} > 0 \tag{13}$$

for all x^* such that $\|y - x^*\| \neq 0$. The sign of $\lambda^*(t)$ can thus be obtained solving (12) using Milstein's method [6]. A brief summary of the method is given in Appendix A.

Milstein's method (presented in Appendix-A) is thus applied to (12), under the assumption that the sensor is a point-mass, and that its associated SDE has constant diffusion coefficient. Note that a full numerical solution of (12) is not required. Comparing (12) to (14) after mapping X to x and Y to λ, suggests that,

$$\begin{aligned} &a(t, x, \bar{w}) = u(t), \ \ f(t, x, \bar{w}) = 0 \Rightarrow b(t, x, \bar{w}) = u(t) \\ &g(t, x, \bar{w}) = \beta\left[(\mu^*)^{\phi^*-1} - 1\right]\frac{\partial \mu^*}{\partial x^*}, \ \ Z(t) = -K^{\intercal}(t), \end{aligned}$$

and the one-dimensional semilinear partial differential equation (PDE) obtained in w for the sensor is

$$\frac{\partial w}{\partial t} + u(t)\,\frac{\partial w}{\partial x^*} + \frac{\sigma^2}{2}\,\frac{\partial^2 w}{\partial x^{*2}} + \beta\left[(\mu^{*\,\phi^*-1} - 1)\right]\frac{\partial \mu^*}{\partial x^*} = 0 \ .$$

Given that $\bar{w}(T) = 0$ as $\lambda^*(T) = 0$, from (15a) it follows that the sign of $\bar{w}(t_{N-1}, x_j)$ depends only on the sign of $g(t_{N-1}, x_j, 0)$—since the first two terms vanish—and given that $\beta > 0$ essentially on the sign of the expression

$$\big[(\mu^*)^{\phi^*-1} - 1\big]\,\frac{\partial \mu^*}{\partial x^*}\bigg|_{t=t_{N-1}} \ .$$

Note now that $\mu^* \geq 1$, and that $\phi^* \equiv \phi(\mu^*) < 1$, which implies that $\mu^{*\,\phi^*-1} - 1 < 0$. Moreover, $\frac{\partial \mu^*}{\partial x^*} > 0$, for $\|y - x^*\| \neq 0$ as indicated in (13), and therefore $\beta\,[\,(\mu^*)^{\phi^*-1} - 1]\frac{\partial \mu^*}{\partial x^*}$ is always negative irrespectively of discretization. In other words, $\bar{w}(t_{N-1}, x_j)$ is negative.

With $\bar{w}(T) = 0$ and $\bar{w}(t_{N-1}, x_j) < 0$, the interpolation in (15b) suggests that $\bar{w}(t_{N-1}, x) < 0$ for all $x \in (x_j, x_{j+1})$. Turning now to (15a) again for $\bar{w}(t_{N-2}, x_j)$ this time, it is seen that the first two terms are nonzero and negative, with the third maintaining its negative sign. It follows that $\bar{w}(t_{N-2}, x)$ is negative, and continuing in this fashion leads to the conclusion that $\bar{w}(t, x) < 0$. Thus without explicitly solving (12), the sign of $\lambda^*(t)$ can be ascertained around any space and time discretization point.

The consequence of having $\lambda^* < 0$ is that the Hamiltonian in (11) is minimized when $u^* = u_{\mathsf{max}}$, which means that the optimal control strategy during interval $[0, T]$ is to close the gap between the sensor and the target as quickly as possible—which is consistent with what has been found for the deterministic case [13]. Thus (10) follows. □

IV. Numerical Results

The optimal control law (10) is applied to (8a) for time $t \in [0, T \wedge T']$, with T' denoting the first exit time from $\|y-x\| > \delta$. Given that what needs to happen is for the sensor to intercept the target as quickly as possible, it makes little sense to continue applying (10) in the δ-ball around y, as this will result to chattering. Instead, once the target is practically intercepted, (8b) allows for the sensor to "smoothly" track its target without overshooting. The complete sensor trajectory for time $t \in [0, T]$ under the switched diffusion (8) is determined by using Euler-Maruyama method [4].

In the numerical single-dimensional (sensor-target distance dynamics) simulation setup the sensor moves with a speed of 50 cm/sec towards a target placed 500 cm away from it in a straight line. Calculations assume $\chi = 1$ cm^2, $\alpha = 10^{-3}$, $\delta = 5$ cm, $k = 10$, and $\beta = 0.167$ counts per second (CPS). Source intensity is taken to be 50 times that of background.

Figure 1 shows the variation of the bound on probability of missed detection as the decision time T increases with noise intensity set at $\sigma = 5$. A gray curve represents the bound for a batch of a single noise realization, and the red curve represents the mean of the bounds over all 100 realizations. The black curve indicates the bound that would have obtained if the sensor motion were deterministic. A simple comparison of the red and black curves suggests that when the sensor motion is noisy, it takes significantly more time for a decision to be reached at the same level of confidence. Before 11 seconds the bound on the probability of false alarm cannot be satisfied so no decision can be made. Figure 2 verifies that in the (time) limit the estimate on the probability of missed detection becomes increasingly more accurate.

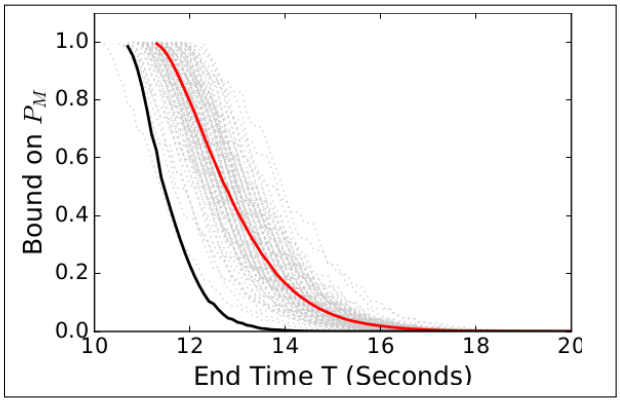

Fig. 1. The estimate of the bound on the probability of missed detection as a function of decision time T.

The next test aims at identifying the effects of noise and source intensity on decision-making accuracy. Toward this end, the diffusion coefficient σ and the ratio of source to background intensity, $\frac{a}{\beta}$, take a range of values. Figures 3 and 4 show how the function that captures the evolution of the bound on the probability of missed detection with the decision time T, varies with increasing noise intensity (Fig. 3) and stronger source compared to background (Fig. 4). Note that as noise increases ($\sigma \uparrow$) or the source intensity decreases ($a \downarrow$), the gap between the deterministic motion Chernoff bound and the stochastic motion bound widens. This indicates that as

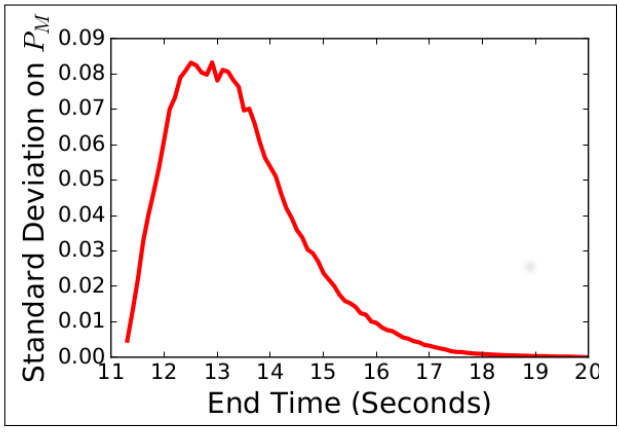

Fig. 2. The standard deviation of the estimate on the bound on probability of missed detection as a function of decision time T.

motion uncertainty increases, or the activity of the source relative to background decreases, increasingly more time is needed to reach a decision with the same confidence as the deterministic case.

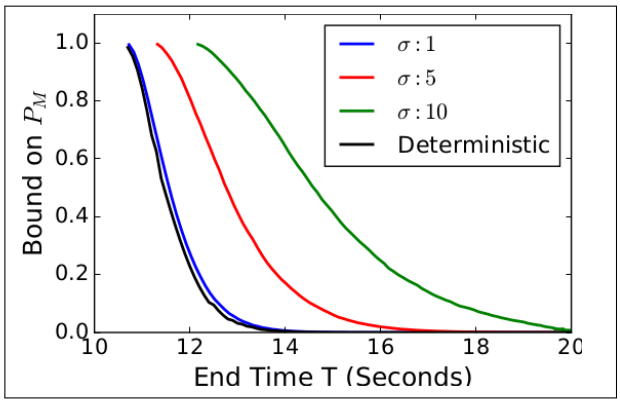

Fig. 3. The evolution of the bound on the probability of missed detection with the decision time deadline for different sensor noise intensities (diffusion coefficients). The (left-most) black curve indicates the bound derived for the deterministic case. All curves correspond to a ratio of source intensity to background equal to 50.

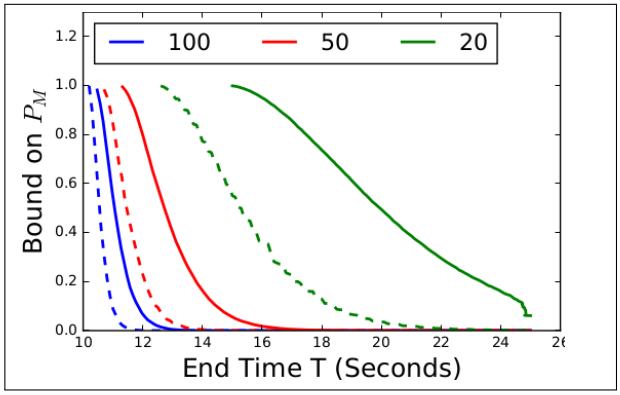

Fig. 4. The bound on the probability of missed detection as a function of the decision time T for different source to background intensity ratios. Dashed curves correspond to the bound for the deterministic case with the same source-to-background ratio as the similarly color-coded stochastic cases. The diffusion coefficient in the equation of motion for the sensor is kept constant at $\sigma = 5$.

V. Conclusions

An analysis based on the stochastic maximum principle reveals that as long as analytically derived Chernoff bounds

on binary hypothesis test error probabilities remain valid and relevant, the sensor coordination strategy that was shown to be optimal in terms of maximizing decision-making accuracy when sensor motion was deterministic, remains optimal when the motion of the sensor is stochastic. Numerical studies further indicate that the noise has a noticeable detrimental effect on decision-making accuracy, which is particularly more pronounced at low source-to-background intensity ratios. Future work is directed to formulating stochastic optimal control laws for networks of sensors, investigation of any possible effects of the choice of the switching parameter δ in the switched diffusion sensor dynamics, and into supporting numerical evidence by experimental results.

APPENDIX

A. Milstein's method

Under some fairly standard smoothness and boundedness conditions on its coefficients [6], the $\mathscr{F}_{t\geq 0}$-adapted solution $\big(X(t), Y(t), Z(t)\big)$ of the coupled FBSDEs

$$\mathrm{d}X = a(t,X,Y)\,\mathrm{d}t + \sigma(t,X,Y)\,\mathrm{d}W \tag{14a}$$

$$\mathrm{d}Y = -g(t,X,Y)\,\mathrm{d}t - f^{\intercal}(t,X,Y)\,\mathrm{d}t + Z^{\intercal}\,\mathrm{d}W \tag{14b}$$

$$X(t_0) = x\ , \qquad Y(T) = \psi\big(X(T)\big) \tag{14c}$$

is unique and related to the solution of the semilinear PDE:

$$\frac{\partial w}{\partial t} + \sum_{i=1}^{d} a^i(t,x,w)\frac{\partial w}{\partial x^i} + \frac{1}{2}\sum_{i,j=1}^{d} a^{ij}(t,x,w)\frac{\partial^2 w}{\partial(x^i)\partial(x^j)} = -g(t,x,w) - \sum_{k=1}^{n} f^k(t,x,w)\sum_{i=1}^{d}\sigma^{ik}(t,x,w)\frac{\partial w}{\partial x^i}$$

where $t < T$, $x \in \mathbb{R}^d$, $w(T,x) = \psi(x)$ and $a^{ij} \triangleq \sum_{k=1}^{d}\sigma^{ik}\sigma^{jk}$. In the single dimensional case, and after setting $b(t,x,y) \triangleq a(t,x,y) + f(t,x,y)\sigma(t,x,y)$, the PDE reduces to

$$\frac{\mathrm{d}w}{\mathrm{d}t} + b(t,x,w)\,\frac{\mathrm{d}w}{\mathrm{d}x} + \frac{1}{2}\sigma^2(t,x,w)\,\frac{\mathrm{d}^2 w}{\mathrm{d}x^2} + g(t,x,w) = 0\ .$$

After defining the constants $h \triangleq \frac{T-t_0}{N}$, $x_j \triangleq x_0 + j\kappa h$, and for $j = 0, \pm 1, \pm 2\ldots$, with $x_j \leq x \leq x_{j+1}$, and $k = N-1, N-2, \ldots, 1, 0$, an approximate solution $\bar{w}(t_k, x)$ of the single-dimensional differential equation can be constructed as

$$\begin{aligned}
&\bar{w}(t_N, x) = \psi(x)\\
&\bar{w}(t_k, x_j) = \frac{1}{2}\bar{w}\Big(t_{k+1},\, x_j + h\,b\big(t_k, x_j, \bar{w}(t_{k+1}, x_j)\big)\\
&\qquad - \sqrt{h}\,\sigma\big(t_k, x_j, \bar{w}(t_{k+1}, x_j)\big)\Big)\\
&\quad + \frac{1}{2}\bar{w}\Big(t_{k+1}, x_j + h\,b\big(t_k, x_j, \bar{w}(t_{k+1}, x_j)\big)\\
&\qquad + \sqrt{h}\,\sigma\big(t_k, x_j, \bar{w}(t_{k+1}, x_j)\big)\Big)\\
&\quad + h\,g\big(t_k, x_j, \bar{w}(t_{k+1}, x_j)\big)
\end{aligned} \tag{15a}$$

$$\bar{w}(t_k, x) = \tfrac{x_{j+1}-x}{\kappa h}\bar{w}(t_k, x_j) + \tfrac{x-x_j}{\kappa h}\bar{w}(t_k, x_{j+1}) \tag{15b}$$

Once $\bar{w}(t_k, x)$ is obtained, and for some $\gamma \approx \sigma(t_k, x)$, the partial derivative of $\bar{w}$ with respect to x at (t_k, x) can be approximated as

$$\frac{\partial \bar{w}}{\partial x}(t_k, x) \approx \frac{\bar{w}(t_k, x+\gamma\sqrt{h}) - \bar{w}(t_k, x-\gamma\sqrt{h})}{2\gamma\sqrt{h}}\ .$$

Setting $\Delta_k W \triangleq W(t_k + h) - W(t_k)$, the numerical solution of (14) at a point x_{k+1} for $k = 0, 1, 2, \ldots$ is then

$$\begin{aligned}
&X_{k+1} = X_k + h\,a\big(t_k, X_k, Y_k\big)\big) + \sigma\big(t_k, X_k, Y_k\big)\,\Delta_k W\\
&Y_k = \bar{w}(t_k, X_k)\\
&X_0 = x\ , \qquad Z_k = \sigma(t, x, \bar{w})\,\frac{\partial \bar{w}}{\partial x}\ .
\end{aligned} \tag{16}$$

REFERENCES

[1] A. Bensoussan. Lectures on stochastic control. 972:1–62, 1982.

[2] Crispin W. Gardiner. *Handbook of stochastic methods : for physics, chemistry and the natural sciences*. Springer series in synergetics. Springer, Berlin, 1983. Includes indexes.

[3] Joseph L. Hibey, Donald L. Snyder, and Jan H. van Schuppen. Error-probability bounds for continuous-time decision problems. *IEEE Transactions on Information Theory*, 24(5):608–622, 1978.

[4] Peter E. Kloeden and Eckhard Platen. *Numerical solution of stochastic differential equations*. Applications of mathematics. Springer, Berlin, New York, 1999.

[5] C. Y. T. Ma, D. K. Y. Yau, N. K. Yip, N. S. V. Rao, and J. Chen. Performance analysis of stochastic network coverage with limited mobility. In *6th IEEE International Conference on Mobile Adhoc and Sensor Systems*, pages 496–505, Oct 2009.

[6] G. N. Milstein and M. V. Tretyakov. Numerical algorithms for forward-backward stochastic differential equations. *SIAM Journal on Scientific Computing*, 28(2):561–582, 2006.

[7] Robert J. Nemzek, Jared S. Dreicer, David C. Torney, and Tony T. Warnock. Distributed sensor networks for detection of mobile radioactive sources. *IEEE Transactions on Nuclear Science*, 51(4):1693–1700, 2004.

[8] Chetan D. Pahlajani, Jianxin Sun, Ioannis Poulakakis, and Herbert G. Tanner. Error probability bounds for nuclear detection: Improving accuracy through controlled mobility. *Automatica*, 50(10):2470–2481, 2014.

[9] N. S. V. Rao, C. W. Glover, M. Shankar, Y. Yang, J. C. Chin, D. K. Y. Yau, C. Y. T. Ma, and S. Sahni. Improved SPRT detection using localization with application to radiation sources. In *12th International Conference on Information Fusion*, pages 633–640, July 2009.

[10] N. S. V. Rao, M. Shankar, J. C. Chin, D. K. Y. Yau, C. Y. T. Ma, Y. Yang, J. C. Hou, X. Xu, and S. Sahni. Localization under random measurements with application to radiation sources. In *11th International Conference on Information Fusion*, pages 1–8, June 2008.

[11] B. Ristic, A. Gunatilaka, and M. Rutten. An information gain driven search for a radioactive point source. In *2007 10th International Conference on Information Fusion*, pages 1–8, July 2007.

[12] Donald L. Snyder. *Random point processes*. Wiley New York, 1975.

[13] Jianxin Sun and Herbert G. Tanner. Constrained decision-making for low-count radiation detection by mobile sensors. *Auton. Robots*, 39(4):519–536, 2015.

[14] H. L. Van Trees, K. L. Bell, and Z. Tian. *Detection Estimation and Modulation Theory, Part I: Detection, Estimation, and Filtering Theory*. Wiley, 2013.